Environment. Technology. Resources. Rezekne, Latvia
Proceedings of the 16th International Scientific and Practical Conference. 2025. Volume IV, 481-488

Determination of Preliminary Operating Power Density Ranges for Some Laser Technological Processes on AISI 316 Stainless Steel

Lyubomir Lazov
Rezekne Academy of Riga Technical University
Rezekne, Latvia
lyubomir.lazov@rta.lv

Nikolay Angelov
Department of Mathematics, Informatics and Natural Sciences Technical University of Gabrovo
Gabrovo, Bulgaria
angelov_np@abv.bg

Erika Teirumnieka
Rezekne Academy of Riga Technical University
Rezekne, Latvia
erika.teirumnieka@rta.lv

Artis Teilans
Rezekne Academy of Riga Technical University
Rezekne, Latvia
artis.teilans@rta.lv

Ritvars Revalds
Rezekne Academy of Riga Technical University
Rezekne, Latvia
ritvars.revalds@rta.lv

***Abstract*—Determination of preliminary operating intervals of power density is the first step in optimizing laser technological processes for AISI 316 stainless steel. The study focuses on the laser technological processes of laser marking, laser cutting, and laser welding. Based on the heat conduction equation and the heat balance equation, calculations were performed to determine the critical power density of melting and vaporization at various speeds for the three processes, taking into account the optical and thermo-physical parameters of the material. The results were graphically presented, analyzed, and summarized. Preliminary operating intervals were determined for laser marking through oxidation, melting, and vaporization, as well as for laser cutting and laser welding at different speeds. Our experimental results, along with results from other authors, showed good agreement with the theoretically defined power density intervals for all three technological processes.**

Keywords – Numerical calculations, laser processes, power density, speed.

I. Introduction

In the last few decades, laser technologies have developed very successfully and are constantly expanding their positions in the industry, gradually displacing a number of traditional technologies [1]. Laser systems are used in production for marking, engraving, cutting, welding, drilling holes, hardening, strengthening, sintering, coating, scribing, etc. [2] - [7]. The optimization of such processes is very complex because research is required for different types of materials, types of lasers used, and laser processing methods. For each specific case, real and numerical experiments are conducted to study the influence of the main parameters on the process in order to obtain the required quality of the products and obtain working intervals of these parameters. Both real and numerical experiments have their advantages and place in the research process for laser technologies:

Real experiments provide insight into laser-material interactions and help improve the optimization of laser technological processes. They allow the observation of key physical phenomena, such as the formation of an oxide layer, melt or channels due to evaporation in the impact zone, the generation of splashes and ridges around the impact zone. They also allow direct measurements to be made of the size of the heat affected zone (HAZ), the depth, width and shape of the channels formed during evaporation, the thickness of the oxide layer, the depth and shape of the melt, the surface roughness, the microhardness, and other possible characteristics of the treated area [8] - [10]. Experiments reveal potential safety issues such as the release of harmful substances, harmful fumes and splashes. Many laser processes include real-time monitoring systems (e.g. thermal cameras, pyrometers or high-speed cameras). These measuring instruments provide valuable feedback during experiments that can be used to dynamically adjust parameters and optimize performance. Practical testing ensures that the desired quality standards are met in real applications.

Numerical experiments are a powerful tool for optimizing laser technology processes. They allow for cost-effective, time-efficient, and detailed analysis of process

Online ISSN 2256-070X
https://doi.org/10.17770/etr2025vol4.8391

parameters and material behaviour. They are highly cost-effective as they eliminate the need for expensive materials, equipment setup, and physical trial-and-error testing. Energy consumption is minimized as many iterations can be performed virtually. They allow testing of new ideas and projects without significant financial investments. In addition, there is a high time efficiency. Simulations allow for systematic variation, analysis and rapid evaluation of various parameters such as laser power, speed, defocus, repetition rate, pulse duration, etc. compared to physical testing [11] - [12]. They provide detailed insight into laser-material interactions such as temperature field distribution and heat transfer, melting and evaporation dynamics, stress and strain during thermal cycling. Numerical experiments provide good predictive capabilities, such as temperature gradients and heat-affected zones (HAZ), material penetration depths, and melting and vaporization thresholds. It is important to provide a safe testing environment when using numerical experiments, avoiding the health risks to researchers associated with working with high-power lasers or hazardous materials.

It is clear that a combined approach of numerical and real experiments provides better opportunities for optimizing laser technological processes [13]. Numerical experiments allow for fast, cost-effective parameter exploration, while real experiments ensure practical feasibility, accuracy and validation of numerical experiments. Together, they create the opportunity for faster optimization and provide reliable, high-quality and efficient results for industrial applications.

In particular, laser technological processes are widely used in industry for marking, welding and cutting steel products. Research on these laser technological processes is constantly developing and enriching, as there are always enough unexplored areas. The quantities and parameters that influence these processes are different, but can be summarized in three groups related to: the properties of the material (optical and thermo-physical), the laser parameters and the parameters of the technological process. For the three processes, power density and speed are very important, as they are of great importance for delivering the necessary energy to the impact zone during their implementation.

The purpose of this study is to determine preliminary operating ranges of power density for different speeds through numerical calculations for the laser technological processes of marking, welding and cutting for AISI 316 steel (1.4404, 10X17H13M2) and their comparison with real experimental studies for these processes.

II. Materials and methods

A. Material

The research is on an austenitic stainless steel AISI 316, which is widely used in industry. It is characterized by high resistance to acids such as sulphuric acid, acetic acid and citric acid, good tensile strength and ductility, excellent weldability with or without filler materials. It uses welded structures operating in highly aggressive environments, designed for long service life at high temperatures. It has a number of marine applications due to its ability to withstand corrosion in salt water, for example, boat fittings and fasteners, marine architecture components such as railings and ladders, submarine parts and shipbuilding. It is suitable for handling aggressive chemicals and is used to make chemical storage tanks, heat exchangers, pumps and valves in chemical processing systems, components for oil and gas extraction. It is also used for the needs of the food industry in the manufacture of brewing and dairy equipment, food processing machinery, cooking equipment and utensils; in the medical and pharmaceutical industries for the manufacture of surgical instruments, medical implants, pharmaceutical manufacturing equipment; architectural applications; power generation facilities; aerospace industry; automotive industry; water purification systems, etc. The chemical composition of the steel is presented in Table 1. It has a high content of chromium, nickel and molybdenum, which significantly increases its corrosion resistance and mechanically robust. It is necessary to emphasize the importance of molybdenum, which contributes to this steel having significant corrosion resistance in environments that are especially rich in chlorides, and in marine environments.

TABLE 1 CHEMICAL COMPOSITION OF AISI 304 STAINLESS STEEL

Element	**Content, %**	**Element**	**Content, %**
C	0.07	Si	< 1.00
Cr	16.50 – 18.50	P	< 0.05
Ni	10.00 – 13.00	S	< 0.02
Mo	2.00 – 2.50	Cu	< 0.30
Mn	< 2.00	Fe	Balance

Some parameters of AISI 316 steel are given in Table 2. It has relatively small values of thermal conductivity and thermal diffusivity coefficients. The heat is retained close to the heat source, which is beneficial in laser welding, laser cutting and laser marking, as this results in a very small heat affected zone (HAZ) ensuring minimal impact on material properties outside the processed area and is very important for machining precision.

TABLE 2 BASIC PARAMETERS OF AISI 316 STAINLESS STEEL

Parameter	**Value**
Absorption capacity A	0.45
Coefficient of thermal conductivity k, W/(kg.K)	16.3
Density ρ, kg/m^3	7970
Specific heat capacity c, J/(kg.K)	510
Coefficient of thermal diffusivity a, m^2/s	4.01×10^{-6}
Melting point temperature T_m, K	1660
Vaporization temperature T_v, K	3084
Latent heat of melting L_m, kJ/kg	273
Latent heat of evaporation L_v, kJ/kg	7450

B. Laser Systems

The calculations apply to laser technology systems that are used in real production.

Laser technology system for marking is with fiber laser, which is a modern laser operating in the near infrared region. The basic parameters of the laser system are given in Table 3. This laser operates in pulsed mode and has a high frequency and pulse duration in the nanosecond range. It has very high beam quality and high efficiency. The laser system is characterized by high positioning accuracy and a high degree of repeatability.

TABLE 3 SOME PARAMETERS OF LASER SYSTEM FOR MARKING

Parameter	**Value**
Wavelength λ, nm	1064
Power P, W	20
Frequency ν, kHz	20 – 50
Pulse duration τ,ns	4 – 200
Pulse energy E_p, mJ	0.1 – 1.0
Pulse power P_p, kW	2.5 – 10
Diameter of work spot d, μm	30
Efficiency, %	40

The laser technological system for welding is with an Nd:YAG laser. This is a solid-state laser emitting in the near infrared region. It operates in pulsed mode. The parameters of the laser system are presented in Table 4. The laser has a low frequency (up to 100 Hz) and a long pulse duration. This makes the laser system suitable for the laser welding process. The positioning accuracy and repeatability of the system are of low values.

TABLE 4 SOME PARAMETERS OF LASER SYSTEM FOR WELDING

Parameter	**Value**
Wavelength λ, nm	1064
Power P, W	500
Frequency ν, Hz	1 – 100
Pulse duration τ,ms	1 – 15
Diameter of work spot d, μm	200
Efficiency, %	40

The laser technological system for cutting is with a fiber laser. This is a laser emitting in the near infrared region. It operates in continuous mode. The parameters of the laser system are presented in Table 5. The positioning accuracy of the laser system is high.

TABLE 5 SOME PARAMETERS OF LASER SYSTEM FOR CUTTING

Parameter	**Value**
Wavelength λ, nm	1064
Operating mode	cw
Power P, W	1000
Diameter of work spot d, μm	100
Efficiency, %	40

C. Methods

As noted, speed v and power density q_s are the most important parameters affecting laser technological processes of marking, cutting and welding.

The impact time on the product and the energy absorbed by the material in the impact zone depend on the speed v. The speed requirements are contradictory: on the one hand, the speed must be high in order to reduce the time required to perform the operation and therefore achieve greater efficiency in the production of the product; on the other hand, it must be relatively low in order to absorb the required amount of energy and reach the required temperature for the implementation of the technological process. Considering the other parameters influencing the processes, it is necessary to find a balance between these conflicting requirements and obtain optimal parameters to achieve high product quality.

The power density q_s of the laser radiation is one of the main parameters that determine the changes in the structure or aggregate state of the material in the impact zone. It must be sufficient to absorb the necessary energy in the material and to obtain oxidation, melting or evaporation depending on the technological process. There is a relationship between the power density q_s, the velocity v and the heating temperature T in the impact zone. For a temperature below the melting point, the formula is used

$$q_s = \frac{k(T - T_0)}{2A}\sqrt{\frac{\pi v}{ad}} \qquad (1)$$

where k is the thermal conductivity coefficient, a – thermal diffusivity coefficient, A – absorption capacity, d – diameter of the working spot, T_0 – initial temperature.

In determining the preliminary operating power density ranges for different speeds, the critical melting and evaporation power densities are used. The formulas are obtained by applying the heat conduction equation and the heat balance equation.

For the critical power density of melting, the formula is obtained

$$q_{scm} = \frac{(1+s)k(T_m - T_0)}{2A}\sqrt{\frac{\pi v}{ad}} \qquad (2)$$

where $s = \frac{L_m}{c(T_m - T_0)}$ (3) is a parameter, L_m – specific heat of melting, c – specific heat capacity.

The formula for the critical power density of evaporation is

$$q_{scv} = \frac{(1+s')k(T_v - T_0)}{2A}\sqrt{\frac{\pi v}{ad}} \qquad (4)$$

where $s' = \frac{L_m + L_v}{c(T_m - T_0)}$ (5) is a parameter, L_v – specific heat of evaporation.

The determination of the intervals of change of the power density for oxidation, melting and evaporation occurs in three stages:

1) Calculation of the critical power density of melting q_{scm} and evaporation q_{scv}.

The values of the critical power densities during melting for different speeds are determined by formula (2),

with the speed changing in a certain interval depending on the technological process. The values of the critical evaporation power densities for different speeds are determined by formula (4). Graphs of the dependences of the critical melting power density on speed and the critical evaporation power density on speed are drawn.

2) Determination of the maximum power density q_{smax} for the laser used.

The maximum power density qsmax is calculated using the formula

$$q_{smax} = \frac{4P_{max}}{\pi d^2} \qquad (6)$$

where P_{max} is the maximum power of the laser.

A separate calculation is made for each laser.

3) Determination of the preliminary power density intervals for oxidation, melting and evaporation for the selected laser and material

The results are presented in a suitable table. The first column shows different speeds, the second column contains the power density intervals for oxidation, the third column for melting, the fourth for evaporation. The third and fourth columns show the power density range. These intervals are clearly shown in the graphical images. The oxidation region is below the graph of the dependence of the critical melting power density on the speed. The melting region is between the two graphs. The evaporation region is above the graph of the dependence of the critical power density of evaporation on the velocity and is limited from above by the maximum laser power density.

Some of our experimental results and the results of other authors are plotted on the graphical images and analyzed for consistency with the theoretical results.

III. Results and Discussion

A. Determining preliminary power density operating intervals for the laser marking process

To determine the critical power density of melting, the parameters from Tables 1, 2 and 3 were used. According to formulas (1) and (2), the critical power density of melting was determined for different speeds for AISI 316 stainless steel. The speed was varied from 10 mm/s to 100 mm/s in 10 mm/s increment. The critical power density of evaporation for different speeds was determined from formulas (3) and (4) as the speed was again varied from 10 mm/s to 100 mm/s in 10 mm/s increments. The results are presented graphically in Figure 1. From the analysis of the graphs it follows:

- With increasing speed, there is a nonlinear increase in the critical power density;
- The critical power density of melting varies from 0.063×10^{10} W/m^2 to 0.198×10^{10} W/m^2 for the studied speed interval;
- The critical power density of evaporation varies from 0.590×10^{10} W/m^2 to 1.867×10^{10} W/m^2 for the studied speed interval. The values of the critical power density of evaporation are about 9.50 times higher than those of the critical power density of melting for the corresponding speed. This is because the vaporization temperature of steel is higher than its melting point. Furthermore, the latent heat of vaporization is significantly higher than the latent heat of melting;
- The curve of critical power density of evaporation is much steeper than the curve of critical power density of melting.

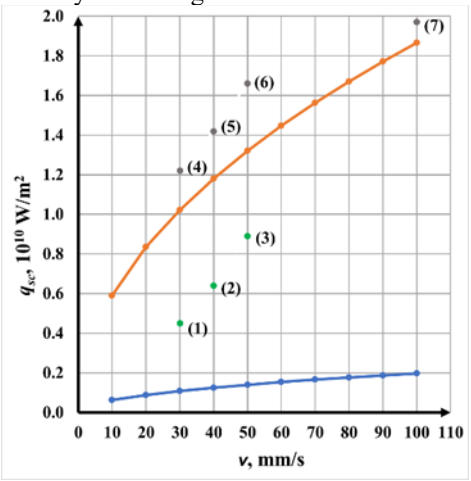

Fig. 1. Graphs of the dependence of the critical power density of melting and evaporation on the speed for AISI 316 steel for the laser marking process.

According to formula (6), the maximum value of the power density of the used laser $q_{smax} = 2.831\times10^{10}$ W/m^2 was determined.

From the obtained results, the preliminary operating intervals of power density for different speeds for AISI 316 steel for the laser marking process by oxidation, melting and evaporation have been determined. The results are presented in Table 6.

TABLE 6 PRELIMINARY OPERATING POWER DENSITY INTERVALS FOR DIFFERENT SPEEDS FOR THE LASER CUTTING PROCESS

***v*, mm/s**	***q*$_s$, W/m^2**		
	Oxidation	***Melting***	***Evaporation***
10	$< 0.063\times10^{10}$	$0.063\times10^{10} - 0.590\times10^{10}$	$0.590\times10^{10} - 2.831\times10^{10}$

v, mm/s	q_s, W/m^2		
	Oxidation	***Melting***	***Evaporation***
20	$< 0.089\times10^{10}$	$0.089\times10^{10} – 0.835\times10^{10}$	$0.835\times10^{10} – 2.831\times10^{10}$
30	$< 0.108\times10^{10}$	$0.108\times10^{10} – 1.022\times10^{10}$	$1.022\times10^{10} – 2.831\times10^{10}$
40	$< 0.125\times10^{10}$	$0.125\times10^{10} – 1.181\times10^{10}$	$1.181\times10^{10} – 2.831\times10^{10}$
50	$< 0.140\times10^{10}$	$0.140\times10^{10} – 1.320\times10^{10}$	$1.320\times10^{10} – 2.831\times10^{10}$
60	$< 0.153\times10^{10}$	$0.153\times10^{10} – 1.446\times10^{10}$	$1.446\times10^{10} – 2.831\times10^{10}$
70	$< 0.166\times10^{10}$	$0.166\times10^{10} – 1.562\times10^{10}$	$1.562\times10^{10} – 0.590\times10^{10}$
80	$< 0.177\times10^{10}$	$0.177\times10^{10} – 1.660\times10^{10}$	$1.660\times10^{10} – 2.831\times10^{10}$
90	$< 0.188\times10^{10}$	$0.188\times10^{10} – 1.771\times10^{10}$	$1.771\times10^{10} – 2.831\times10^{10}$
100	$< 0.198\times10^{10}$	$0.198\times10^{10} – 1.867\times10^{10}$	$1.867\times10^{10} – 2.831\times10^{10}$

We conducted experimental studies on the process of laser marking of AISI 316 stainless steel samples with a fiber laser. Experimental results are presented with green and gray dots in Fig. 1, marked with numbers. These are the parameters that relate to the obtained markings:

for laser marking by melting

Areas are marked with: (1) – $q_s = 0.45\times10^{10}$ W/m^2 and $v = 30$ mm/s, (2) – $q_s = 0.64\times10^{10}$ W/m^2 and $v = 40$ mm/s, and (3) – $q_s = 0.89\times10^{10}$ W/m^2 and $v = 50$ mm/s. The markings are of high contrast, which ranges from 72 % to 67 %.

A good correlation is observed between the experimental values of these regions and the theoretically obtained melting zone located between the two plots in Fig. 1. All green dots are located in this zone.

for laser marking by evaporation

Areas are marked with: (4) – $q_s = 1.22\times10^{10}$ W/m^2 and $v = 30$ mm/s, (5) – $q_s = 1.42\times10^{10}$ W/m^2 and $v = 40$ mm/s, and (6) – $q_s = 1.66\times10^{10}$ W/m^2 and $v = 50$ mm/s. The markings are of high contrast, which ranges from 81 % to 75 %.

All these gray points in Fig. 1 are located above the graph of the theoretical dependence of the critical power density of evaporation on the speed for the studied steel. The experimental data and the preliminary operating intervals of power density for different speeds are consistent.

Some authors also obtain values of power density and speed parameters, which are consistent with the obtained preliminary operating intervals of power density. In the publication of [14], the authors implement laser marking by evaporation with a contrast of the marked area of 79 % at $q_s = 1.97\times10^{10}$ W/m^2 and $v = 100$ mm/s, which corresponds to point number (7) in Fig. 1. The experiments were performed with a fiber laser and for steel 75, which has similar characteristics to those of AISI 316 steel. In article [15], the authors obtain experimental results that are consistent with preliminary operating intervals of power density.

B. Determination of preliminary operating intervals of power density for the laser cutting process

To determine the critical power density of melting and evaporation for AISI 316 stainless steel, the parameters from Tables 1, 2 and 5 were used. Again, as in marking, formulas (1), (2), (3) and (4) are used, with the speed varying from 10 mm/s to 100 mm/s in steps of 10 mm/s. From the obtained numerical calculations, graphs of the dependence of the critical power density of melting and evaporation on the speed for the studied steel for laser cutting were constructed. The following conclusions can be drawn from the graphs:

- A nonlinear increase in the critical power density with increasing speed is observed for the laser cutting process;
- The critical power density of melting is in the interval from 0.034×10^{10} W/m^2 to 0.108×10^{10} W/m^2 for a velocity change from 10 mm/s to 100 mm/s. The critical power density of evaporation varies from 0.323×10^{10} W/m^2 to 1.022×10^{10} W/m^2 for the investigated velocity interval. Again, the critical power density of evaporation is significantly higher;
- The rate of change of the critical power density of evaporation is 7.77×10^7 (W/m^2)/(mm/s), while for

the critical power density of melting it is 0.822×10^7 (W/m^2)/(mm/s).

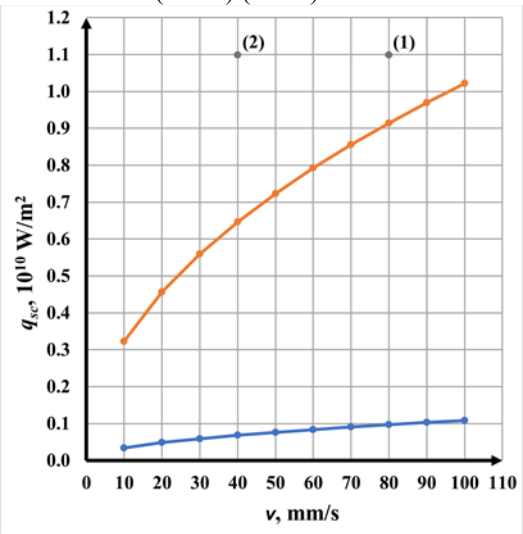

Fig. 2. Graphs of the dependence of the critical power density of melting and evaporation on the speed for AISI 316 steel for the laser cutting process

According to formula (6), the maximum value of the power density of the used laser $q_{smax} = 12.74\times10^{11}$ W/m^2 was determined.

From the obtained results, the preliminary operating intervals of power density for different speeds for AISI 316 steel for the laser cutting process have been determined. The results are presented in Table 7.

TABLE 7 PRELIMINARY OPERATING POWER DENSITY INTERVALS FOR DIFFERENT SPEEDS FOR THE LASER CUTTING PROCESS

v, mm/s	q_s, W/m^2
10	$0.323\times10^{10} - 12.74\times10^{11}$
20	$0.457\times10^{10} - 12.74\times10^{11}$
30	$0.560\times10^{10} - 12.74\times10^{11}$
40	$0.647\times10^{10} - 12.74\times10^{11}$
50	$0.723\times10^{10} - 12.74\times10^{11}$
60	$0.792\times10^{10} - 12.74\times10^{11}$
70	$0.856\times10^{10} - 12.74\times10^{11}$
80	$0.915\times10^{10} - 12.74\times10^{11}$
90	$0.970\times10^{10} - 12.74\times10^{11}$
100	$1.022\times10^{10} - 12.74\times10^{11}$

In the paper [16], the authors investigated the effect of speed at different power densities for cutting AISI 316 steel samples with a fiber laser. The following results were obtained: cutting a 3 mm thick sample with $q_s = 1.11\times10^{10}$ W/m^2 and $v = 80$ mm/s (see point (1) of Fig. 2), and cutting a 4 mm thick sample with $q_s = 1.11\times10^{10}$ W/m^2 and $v = 40$ mm/s (see point (2) of Fig. 2). They are located above the theoretical graph of the dependence of the critical power density of evaporation on speed and laser cutting by evaporation is realized.

C. Determination of preliminary operating intervals of power density for the laser welding process

In the numerical calculations for the laser welding process of AISI 316 stainless steel, the parameters from Tables 1, 2 and 4 were used. Again, as in the other two processes, formulas (1), (2), (3) and (4) were used, with the speed varying from 30 mm/s to 300 mm/s in steps of 10 mm/s. From the obtained numerical calculations, graphs of the dependence of the critical power density of melting and evaporation on the speed for the studied steel for laser welding were constructed. From the analysis of the graphs, the following conclusions can be drawn:

- A nonlinear increase in the critical power density with increasing speed is observed for the laser welding process;
- The critical power density of melting is in the interval from 0.042×10^{10} W/m^2 to 0.133×10^{10} W/m^2 for the speed range from 30 mm/s to 300 mm/s. The critical power density of evaporation varies from 0.396×10^{10} W/m^2 to 1.252×10^{10} W/m^2 for the studied speed interval;
- The rate of change of the critical power density of evaporation is 3.17×10^7 (W/m^2)/(mm/s), while for the critical power density of melting it is 0.337×10^7 (W/m^2)/(mm/s).

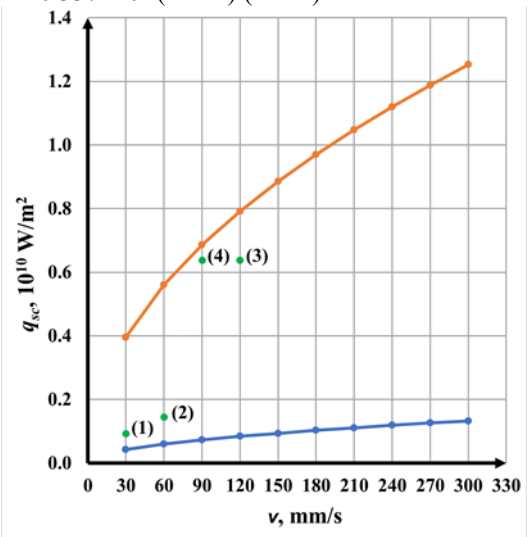

Fig. 3. Graphs of the dependence of the critical power density of melting and evaporation on the speed for AISI 316 steel for the laser welding process

According to formula (6), the maximum value of the power density of the used laser $q_{smax} = 1.592\times10^{10}$ W/m^2 was determined.

From the obtained results, the preliminary operating intervals of power density for different speeds for AISI 316 steel for the laser welding process have been determined. The results are presented in Table 8.

TABLE 8 PRELIMINARY OPERATING POWER DENSITY INTERVALS FOR DIFFERENT SPEEDS FOR THE LASER WELDING PROCESS

v, mm/s	q_s, W/m^2
30	$0.042\times10^{10} – 0.396\times10^{10}$
60	$0.050\times10^{10} – 0.560\times10^{10}$
90	$0.073\times10^{10} – 0.686\times10^{10}$
120	$0.084\times10^{10} – 0.792\times10^{10}$
150	$0.094\times10^{10} – 0.886\times10^{10}$
180	$0.103\times10^{10} – 0.970\times10^{10}$
210	$0.111\times10^{10} – 1.048\times10^{10}$
240	$0.119\times10^{10} – 1.120\times10^{10}$
270	$0.126\times10^{10} – 1.188\times10^{10}$
300	$0.133\times10^{10} – 1.252\times10^{10}$

We conducted experimental studies with a laser system with a diode laser “DF 025” with a wavelength of 808 nm, operating in cw mode. We obtained high-quality laser welding with the following parameters: speed 30 mm/s and power density 9.36×10^8 W/m^2 (see point (1) of Fig. 3) and speed 60 mm/s and power density 14.5×10^8 W/m^2 (see point (2) of Fig. 3). As can be seen from Fig. 3, these points are located between the two curves, which corresponds to a region in which the material is melted. Therefore, there is a complete correspondence between theoretical and experimental results.

In [17], the author Renald Schedewy investigated the laser welding process with a fiber laser on structural steel. The results he obtained were: a weld depth of 2.5 mm at 6.37×10^9 W/m^2 and a speed of 120 mm/s (see point (3) of Fig. 3) and a weld depth of 2.9 mm at 6.37×10^9 W/m^2 and a speed of 90 mm/s (see point (4) of Fig. 3).

IV. CONCLUSIONS

The conducted researches have established the following results:

- Preliminary working intervals of power density were determined for different speeds for different marking methods: by oxidation, which requires lower power density; by melting, which operates at a relatively high power density; by evaporation, which requires even higher power density;
- Preliminary working intervals of power density were determined for different speeds for laser cutting;
- Preliminary working intervals of power density were determined for different speeds for laser welding;
- Consistency of the obtained theoretical results with our and other authors' experimental results was obtained.

The research is a first stage of the optimization of these technological processes on AISI 316 stainless steel. They should continue with experimental and theoretical studies on frequency, pulse duration, effective energy, defocus, etc. The results are of assistance to designers and operators of laser technological systems.

REFERENCES

[1] W. Khan, R. Yasmin, H. Akbar, Eds., Laser Technology: Bridging Historical Milestones and Modern Applications in Science, Industry, and Sustainability, Global Scientific and Academic Research Journal of Multidisciplinary Studies, 2025, pp. 70-84, DOI: 10.5281/zenodo.14770605

[2] M. Chau, "An Overview Study on the Laser Technology and Applications in the Mechanical and Machine Manufacturing Industry," Journal of Mechanical Engineering Research and Developments, 42(5):16-20, August 2019, DOI: 10.26480/jmerd.05.2019.16.20

[3] L. Legres, C. Chamot, M. Varna, A. Janin, "The Laser Technology: New Trends in Biology and Medicine," Journal of Modern Physics, 5(05): 267-279, March 2014, DOI: 10.4236/jmp.2014.55037

[4] A. Stepanov, E. Saukkonen, H. Piilia, Possibilities of laser processing of paper materials, 15th Nordic Laser Materials Processing Conference, Nolamp 15, 25-27 August 2015, Lappeenranta, Finland, Physics Procedia, 78: 138 – 146, 2015, DOI: 10.1016/j.phpro.2015.11.026

[5] T. Ness, "Applications and Advantages of Fiber Laser Technology in the Automotive and Aerospace Industries," International Photonics and Optoelectronics Meetings OSA Technical Digest (online), (Optica Publishing Group, , paper MTh3A.2, 2012, https://doi.org/10.1364/LTST.2012.MTh3A.2

[6] X. Zhang, L. Zhou and G. Feng, "Laser technologies in manufacturing functional materials and applications of machine learning-assisted design and fabrication, " Advanced Composites and Hybrid Materials, 8:76, 2025, https://doi.org/10.1007/s42114-024-01154-4

[7] K. Zhou, S. Sang, C. Wang and Y. Zhou, "Principle, Application and Development Trend of Laser Cleaning, " MMEAT-2022, Journal of Physics: Conference Series, 2383, 012075, 2022, DOI: 10.1088/1742-6596/2383/1/012075

[8] M. Kutsuna and S. Marya, Research and development of laser technology in materials processing, Proceedings of SPIE - The International Society for Optical Engineering, March 2003, 4831:104-109, 2003, DOI:10.1117/12.497939

[9] X. Wang, J. Takács J., G. Krallics and A. Szilagyi, "Experimental research on laser-material interaction, " Periodica Polytechnica Transportation Engineering 28(1), January 2001, https://www.researchgate.net/publication/242194826_Experimental_research_on_laser-material_interaction

[10] M. Pandey and B. Doloi, "Experimental Studies on Laser Marking Characteristics of Stainless Steel 304, " Advances in Modern Machining Processes, 173-184, December 2022, DOI: 10.1007/978-981-19-7150-1_15

[11] O. Ganzulenko and A. Petkova, "Simulation and approbation of the marking laser process on metal materials, " Journal of Physics

Conference Series, 1753(1):012016, February 2021, DOI:10.1088/1742-6596/1753/1/012016

[12] S. Tsirkas, P. Papanikos and T. Kermanidis, "Numerical Simulation of the Laser Welding Process in Butt-Joint Specimens, " Journal of Materials Processing Technology, 134(1):59-69, March 2003, DOI:10.1016/S0924-0136(02)00921-4

[13] G. Rodrigues, J. Pencinovsky, M. Cuypers and J. Duflou, "Theoretical and experimental aspects of laser cutting with a direct diode laser, " Optics and Lasers in Engineering, 61:31–38, October 2014, DOI: 10.1016/j.optlaseng.2014.04.013

[14] P. Tsvyatkov, E. Yankov, L. Lazov and E. Teirumnieks, Investigation of the Influence of Technological Parameters of Laser Marking on the Degree of Contrast, Environment. Technology. Resources. Rezekne, Latvia, Proceedings of the 14th International Scientific and Practical Conference, Volume 3, 370-374, 2024, DOI:10.17770/etr2023vol3.7319

[15] L. Lazov, E. Teirumnieks, Ts. Karadzhov and N. Angelov, "Influence of power density and frequency of the process of laser marking of steel products, " Infrared Physics & Technology, Volume 116, 103783, August 2021, DOI: https://doi.org/10.1016/j.infrared.2021.103783

[16] A. Wetzig, P. Herwig and J. Hauptmann, "Latest Developments of Laser Cutting, " Paper 103, pp. 1-10, https://publica-rest.fraunhofer.de/server/api/core/bitstreams/5e759d65-3018-40c3-94b3-e1409babad52/content

[17] Fraunhofer – Institut fur Werkstoff und Strahltechnik, Jahresbericht 2009, Dresden, 2009, https://www.JB_IWS_2009_de%20(2).pdf